Experimental demonstration of controllable double magneto-optical traps on an atom chip

Hui Yan,[1,2,3,4] Guo-Qing Yang,[1,2,3] Tao Shi,[1,2,3] Jin Wang,[1,2,*] and Ming-Sheng Zhan[1,2]

[1]*State Key Laboratory of Magnetic Resonance and Atomic and Molecular Physics, Wuhan Institute of Physics and Mathematics, Chinese Academy of Sciences, Wuhan 430071, China*
[2]*Center for Cold Atom Physics, Chinese Academy of Sciences, Wuhan 430071, China*
[3]*Graduate School, Chinese Academy of Sciences, Beijing 100080, China*
[4]*yanhui@wipm.ac.cn*
*Corresponding author: wangjin@wipm.ac.cn

We demonstrate controllable double magneto-optical traps (DMOTs) on an atom chip: At first, DMOTs, which trap atoms directly from the background rubidium vapor in an ultrahigh-vacuum environment, are realized on an atom chip simultaneously. The double quadrupole magnetic fields are produced by two separate U-shaped microwires on the atom chip, combined with a bias magnetic field. Then, we determine the best parameters for a U-shaped magneto-optical trap (UMOT) through a detailed comparison of the capture ability at different currents and the bias magnetic field between two different geometric sizes of UMOT. Finally, we demonstrate the mixing and splitting of the DMOTs on the atom chip with the help of an extra pair of anti-Helmholtz coils.
© 2008 Optical Society of America

OCIS codes: 020.0020, 020.7010, 020.7490, 230.3990.

Currently, the atom chip is attracting more and more interest because of its inherent advantages of integration and miniaturization. Not only can all the traditional cold atom experiments be transferred to the atom chip, but also many novel applications have been proposed and realized [1,2], for example, theoretical or experimental research about controllable double magneto-optical traps (DMOTs) [3–5], two species surface MOTs [6,7], stable double magnetic traps [8], or even multiple MOTs [9] and multiple traps [10–13]. Here we focus on controllable DMOTs for the following reasons: First, they are the basis for double magnetic traps and independent double Bose–Einstein condensates (BECs) [8,14–17]. On the other hand, DMOTs are so close to each other that they provide a good physical system for studying cold collisions between different samples, including, for example, two isotope samples [6,7,18]. Furthermore, they could also be applied to the study of entanglement between different atom assemblies [19,20] and even quantum registers for quantum computation and quantum teleportation [21–23]. In this paper, we describe how we have realized controllable DMOTs on our homemade atom chip experimentally. Compared with the original experimental works, such as two and multiple atom traps on an atom chip [8,10–13], our DMOTs have the further advantage of directly trapping atoms from the background Rb vapor with the atom chip, without requiring a transfer from any other kind of trap, such as a mirror MOT or a Z trap. Furthermore, through a detailed comparison of the capture ability at different currents and the bias magnetic field between two different geometric sizes of U-shaped MOT (UMOT), we determine the best parameters for a UMOT [24,25].

Hence the DMOTs are optimized and the number of trapped atoms is more than 10^6 in each trap of our DMOTs. Thus the results will also be helpful for a UMOT or multiple UMOT design on an atom chip. In addition, we demonstrate the mixing and splitting of the DMOTs on the atom chip with the help of an extra pair of anti-Helmholtz coils in the experiment.

Our atom chip is manufactured by combining the wet etching method with electroplating techniques [26]. After fabrication, the atom chip is placed in an ultrahigh vacuum with a glass cell. The wire structure on the atom chip is shown in Fig. 1. Double dark U-shaped wires are
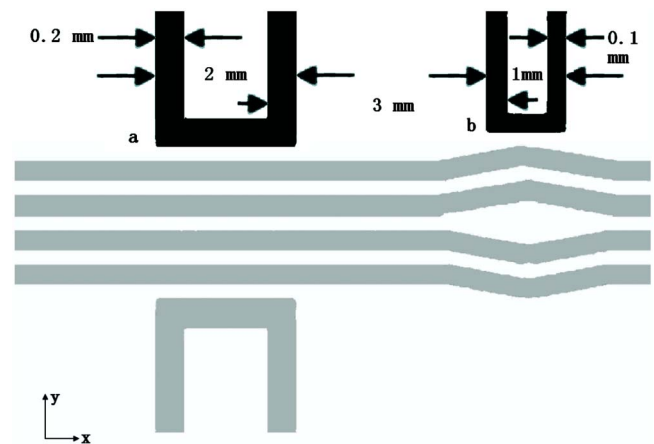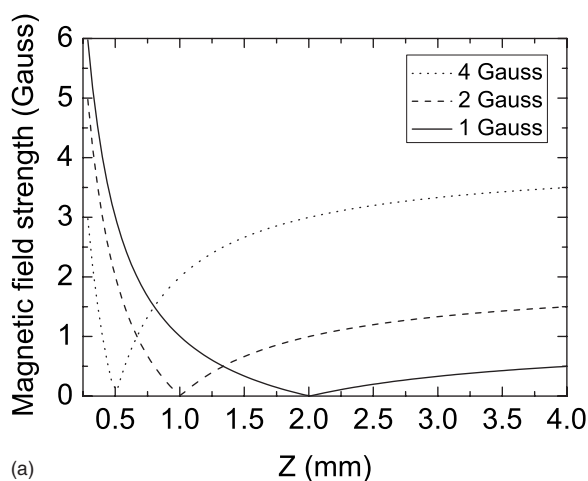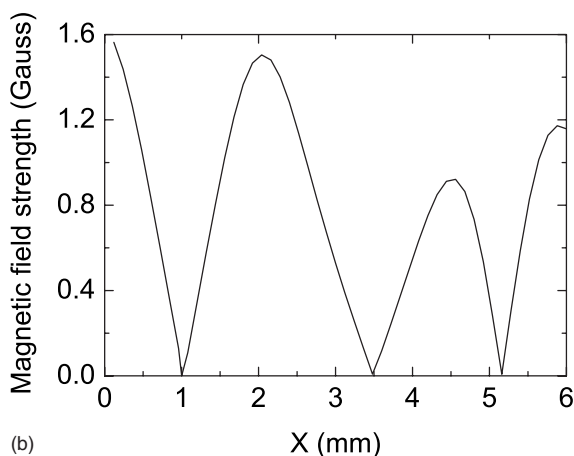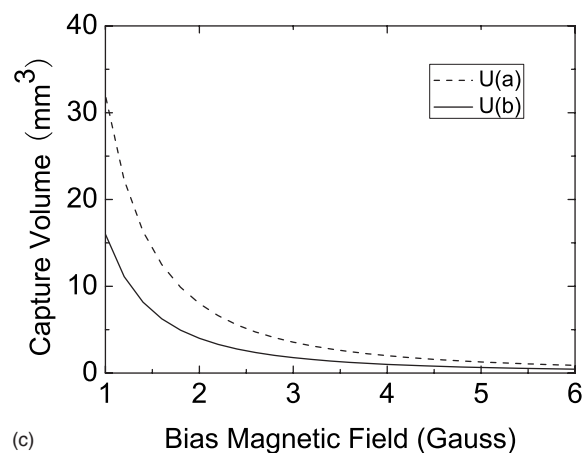

Fig. 1. (Color online) Wire diagram of our atom chip, including U-shaped traps, guiding wires, double Y-shaped splitting and combining wires. Only the double dark U-shaped wires (a, b) are used in the present experiment.

(a)

(b)

(c)

Fig. 2. Magnetic field distribution and capture volume of the double MOTs. (a) Z direction magnetic field distribution, $I = 1$ A, $B_{bias} = 1$ G, 2 G, 4 G. (b) X direction magnetic field distribution, $I = 1$ A. (c) Capture volumes versus different bias magnetic fields; the dashed curve refers to the U(a) MOT and the solid curve refers to the U(b) MOT.

used in the present experiment. The wire width of U(a) is 0.2 mm and that of U(b) is 0.1 mm. The lengths in the X direction of the double U-shaped wires are 2 and 1 mm, respectively. The double U-shaped wires are 3 mm apart from each other. To compare and test the capture ability of the double UMOTs, we calculate the field distributions
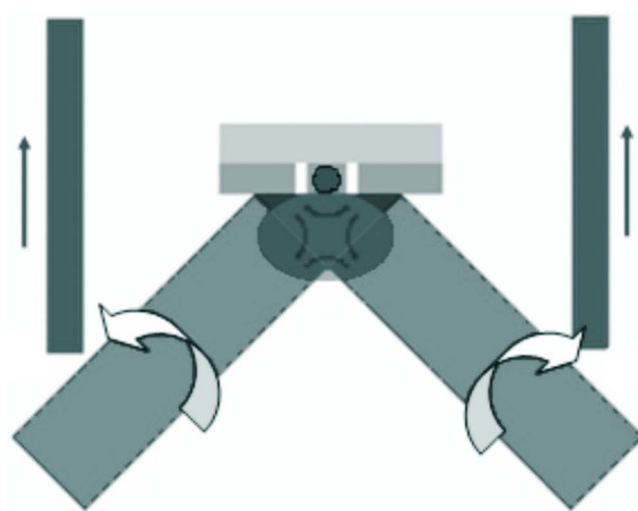

Fig. 3. (Color online) Experimental setup of the double MOTs; it is the same as for a normal UMOT. Two pairs of laser beams are used; one pair is propagated in the plane of the atom chip, and the other pair is reflected by the chip at an angle of 45°. The double microquadrupole magnetic fields are provided by two U-shaped wires on the chip and an extra bias magnetic field that is provided by a pair of Helmholtz coils.

and capture volumes of the DMOTs in theory at first. A simple formula is selected to describe the quadrupole magnetic field:

$$B = \mu_0 I/2\pi r + \vec{B}_{bias}, \qquad (1)$$

where μ_0 is the susceptibility of vacuum, I is the operating current, r is the radial distance from the wire, and $\vec{B}_{bias}$ is the horizontal bias magnetic field. From Eq. (1), the three-dimensional magnetic distributions can be calculated. The result is shown in Fig. 2. Figure 2(a) is the magnetic distribution in the Z direction with different bias fields. The currents in both U-shaped wires are selected to be 1 A, which is the largest current we can use in the experiment in order to protect the U(b) wire from overheating. Figure 2(b) is the magnetic field distribution in the X direction. Although the capture volume is determined by the capture lengths in three dimensions, the capture length in the Y direction can be assumed to be the same as in the Z direction, so a simple equation {$V = [(\mu_0 I)/(\pi B_{bias})]^2 \cdot L$, where L is the lengths in the X direction} can be used to describe the capture volume. Then we obtain the capture volume of the double MOTs as shown in Fig. 2(c). The capture volume of U(a) is almost twice as large as that of U(b) because the lengths in the X direction of the U-shaped wires are not the same in each case.

The experimental setup of the double MOTs is shown in Fig. 3. Two pairs of laser beams are used to trap the atoms. The configuration is the same as a normal UMOT [24,27]. Just two pairs of laser beams are needed in the experiment. One pair of laser beams is propagated in the plane of the chip, and the other pair is reflected by the chip surface at an angle of 45°. The double micro quadrupole magnetic fields are provided by two U-shaped wires on the chip, the axis of the double micro quadrupole magnetic fields also being tilted by 45° with respect to the mirror surface. An extra bias magnetic field is applied by a
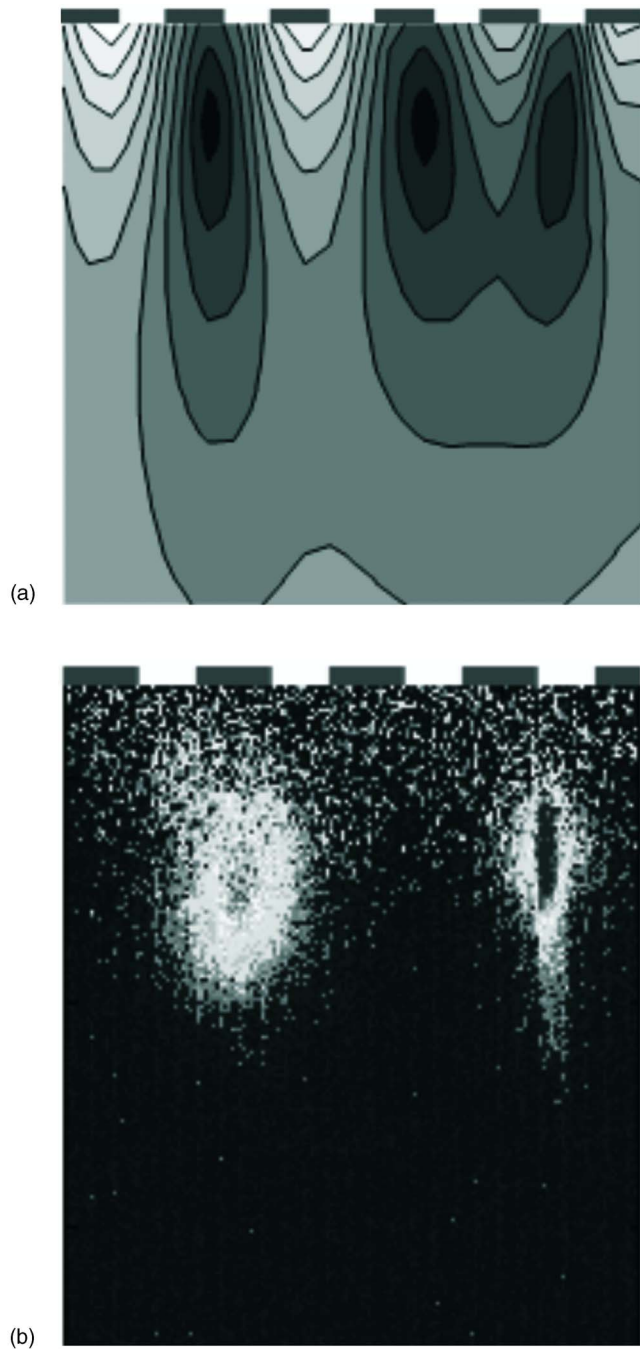
(a)

(b)

Fig. 4. (Color online) (a) Magnetic field distribution in the *XZ* plane. There are three quadrupole magnetic fields in the *XZ* plane, but the center one does not satisfy the MOT condition. (b) Fluorescence picture of the double MOT. The dashed lines on the top of both figures represent the position of the atom chip.

pair of Helmholtz coils. The diameter of the laser beams is 1 cm and the intensity is 9 mW/cm^2. The detuning of the cooling laser frequency is set to 13 MHz redshift with respect to the atomic resonance ^{85}Rb: $5S_{1/2}$, $F=3\rightarrow5P_{3/2}$, $F=4$. The power of the repumping laser is 6 mW, and its frequency is tuned to the resonance ^{85}Rb: $5S_{1/2}$, $F=2$ $\rightarrow5P_{3/2}$, $F=3$.

A Rb dispenser is used to produce atomic vapor. We first applied an intense current (5 A) on the dispenser to emit enough rubidium vapor and increase the vacuum

from 1×10^{-7} to 8×10^{-6} Pa; then we kept this pressure during the experiment by reducing the current to 4 A. An ordinary CCD camera is used to monitor the atomic fluorescence of the trap area, and a digital CCD and image lenses are used to take the fluorescence picture and to measure the number of trapped atoms.

From Eq. (1) we know that the stronger the current we use, the bigger the capture volume we get. However, to protect both U-shaped wires, we select 1 A for both of them, this being the largest value that does not lead to thermal breakdown of the U(b) wire. We select the same current for both wires in order to evaluate the capture volume. When the bias field is set to 1 G, the capture volume of U(a) is approximately 40 mm^3; the field gradient is 5 G/cm. As shown in Fig. 4(b), the DMOTs are realized simultaneously. This observation corresponds well to the theoretical calculation of the magnetic field distribution, shown in Fig. 4(a). The central quadrupole magnetic field does not satisfy the MOT condition in both the magnetic field direction and laser beam polarization. The DMOT wells are thus 4 mm apart from each other (center to center) and 2 mm below the atom chip surface. As shown in Fig. 5(a), the diameter of the U(a) MOT is approximately 1.5 mm, and the total number of trapped atoms is approximately 2×10^6. The diameter of the U(b) MOT is approximately 0.8 mm, and the total number of trapped atoms is approximately 1×10^6, as Fig. 5(b) shows. Thus, the number of atoms in the U(a) MOT is almost twice the number in the U(b) MOT. This coincides well with theory, as shown in Fig. 2(c). Furthermore, as shown in the left
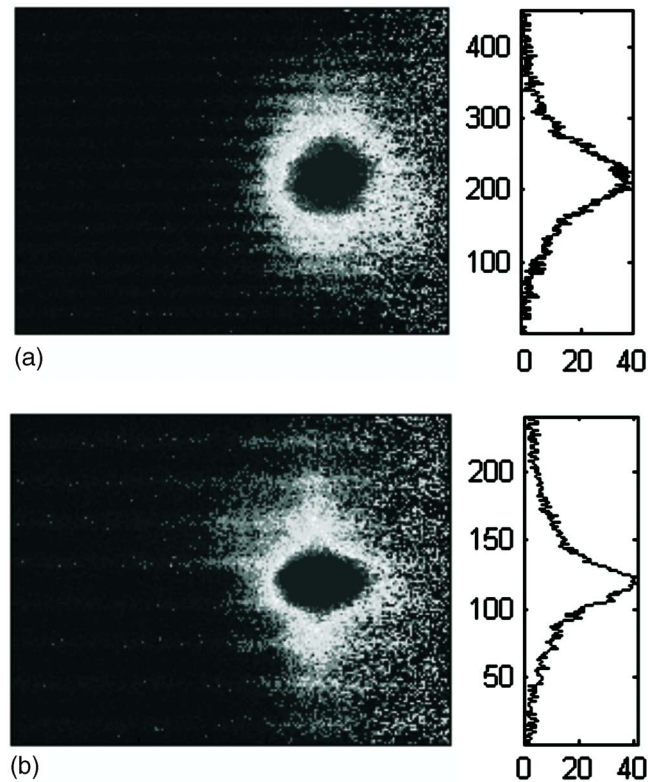

(a)

(b)

Fig. 5. (Color online) (a) Fluorescence picture (left) and *X* direction density distribution (right) of the cold atoms in the U(a) MOT. (b) Fluorescence picture (left) and *X* direction density distribution (right) of cold atoms in the U(b) MOT.
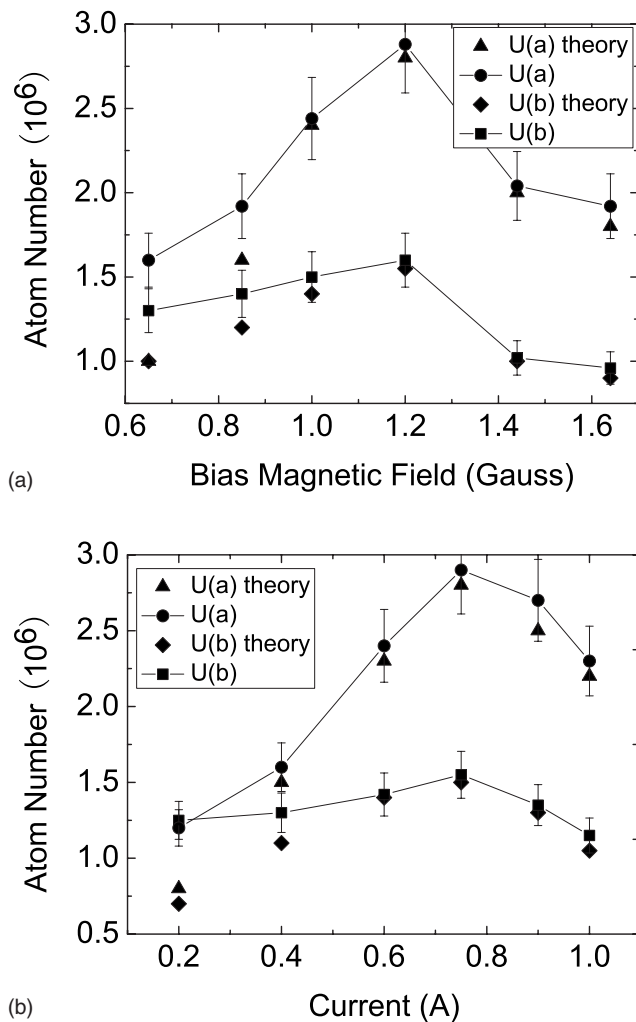
(a)

(b)

Fig. 6. (a) Experimental (dots and squares) and theoretical (triangles and rhombuses) trapped atom numbers versus different bias magnetic fields for the DMOTs. The current is settled at 0.8 A. (b) Experimental and theoretical trapped atom numbers versus different currents in the wires for the DMOTs. The bias magnetic field is settled at 1.2 G.

picture of Fig. 5, the density distributions of both MOTs are of typical Gaussian form. The temperature of the DMOTs is measured to be 300 μK by the time-of-flight (TOF) method.

To evaluate the capture ability and optimize the DMOTs, we measure the trapped atom number under different conditions. As shown in Fig. 6(a), when keeping the currents stable at 0.8 A and altering the bias magnetic field, a 1.2 G bias magnetic field is the best choice for both MOTs. Then keeping the bias magnetic field at 1.2 Gauss,

the trapped atom number versus different currents is shown in Fig. 6(b). Furthermore, we do a brief quantitative calculation about the trapped atom number $\{N = (\alpha/\sqrt{6}\sigma)(V^{2/3}/v_c^4)[m/(2k_BT)]\}^2$, where V is the capture volume, v_c is the smallest capture velocity of the three directions, σ is the collision cross index, $\alpha = I/I_{sat.}$ is the saturated index, k_B is the Boltzmann constant, m is the atomic mass, and T is the temperature of the background atoms) [5]. The results agree well with the experimental results as shown in Fig. 6. From both the experiments and the quantitative calculation, we obtain that the field gradient $(2\pi B_{bias}^2/\mu_o I)$ equals 10 G/cm is the best choice for the DMOTs. Thus $B_{bias} = \sqrt{\mu_0 I/20\pi}$ is the best parameter for a UMOT. This ratio between the current and the bias magnetic field gives the best balance of the capture volume and the magnetic field gradient for the DMOTs because increasing one of those two parameters will decrease the other one at the same time and an efficient MOT always needs large values of those two parameters. In addition, from Fig. 6 we also note when a small current or a small bias magnetic field makes a comparative capture ability of the two different sizes of UMOT. This is determined by the field gradient in the X direction and for the reason that when the field gradient in the X direction is smaller than the other directions (10 G/cm), then the larger length will give a smaller field gradient, and hence affect the capture ability. Thus the U(b) can trap the same or even more atoms as the U(a). Thus we can get another optimized parameter for the UMOT ($L_X = 20B_{bias}$). For example, when the current is 1 A in the U-shaped wire, the best bias magnetic field is 1.4 G and the best length in the X direction (L_X) is 2.8 mm. These two are the basic parameters in a UMOT design.

As Fig. 7 shows, the DMOTs can also be mixed and split with the help of an extra pair of anti-Helmholtz coils. This pair of anti-Helmholtz coils whose center is located in the middle of the DMOTs is used to trap the mirror MOT, and it can provide a 2 G/cm gradient field with a 1 A current. When the DMOTs are realized, we increase the currents in these coils from 0 to 5 A slowly and detect the mixing process of the DMOTs, as shown in Fig. 8(a). Then we decrease the currents from 5 to 0 A slowly, and the MOT is split back into the DMOTs, as shown in Fig. 8(b). Then we increase the currents step by step and measure the split distance, as shown in Fig. 9.

Furthermore, this scheme for realizing double MOTs can be easily extended to 1D or 2D arrays of surface MOTs or used to prepare a 1D or 2D MOT lattice [9]. For example, if an array of U-shaped wires is fabricated on a chip, then with exactly the same configuration of laser beams, an array of UMOTs can be realized simultaneously. When altering the optical beams from a
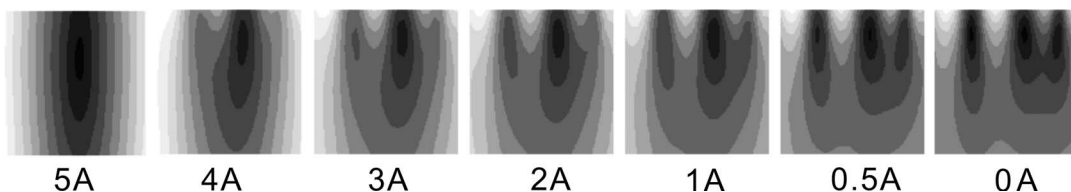

| 5A | 4A | 3A | 2A | 1A | 0.5A | 0 A |

Fig. 7. Magnetic field distributions versus different currents in the extra pair of anti-Helmholtz coils.

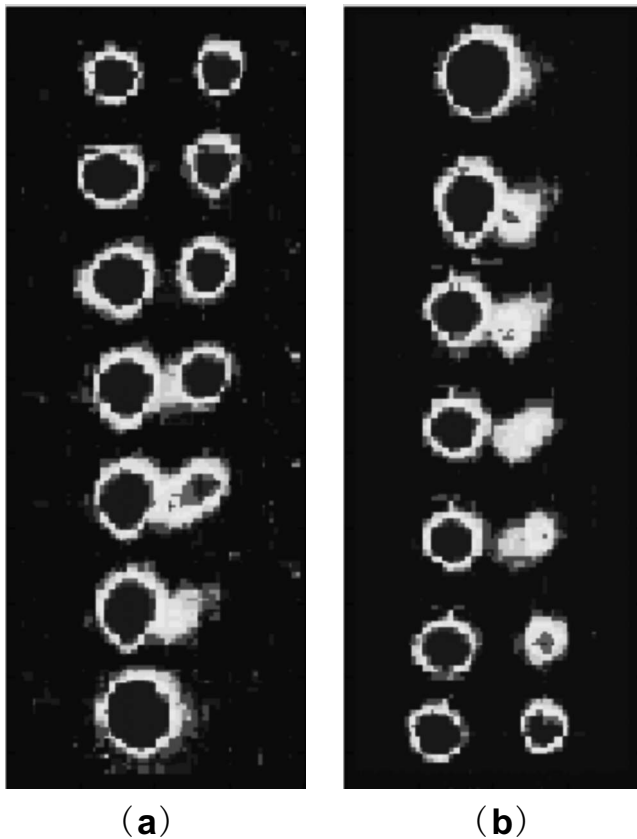(**a**)   (**b**)

Fig. 8.   (a) Mixing of the DMOTs, (b) splitting of the DMOTs.
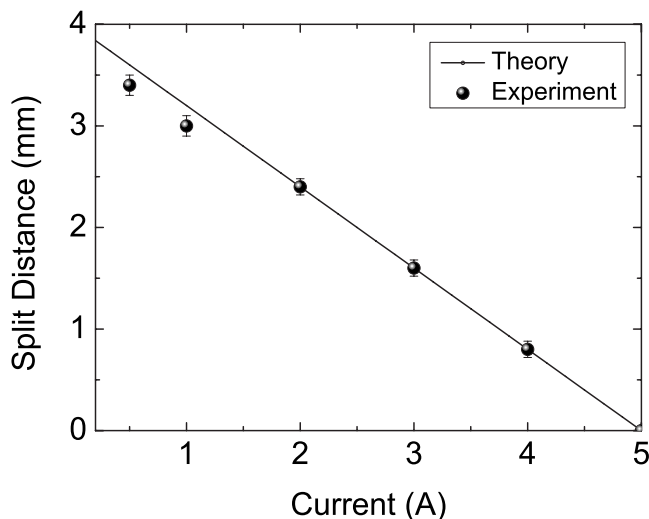

Fig. 9.   Separation distances versus different currents in the extra pair of anti-Helmholtz coils; the dots are the experimental result, and the line is the theoretical result.

Gaussian beam to a plane beam, all the UMOTs will have the same capture efficiency.

In conclusion, we have demonstrated the realization of DMOTs on an atom chip experimentally, and the results coincide well with the theory. In addition, we find out the optimized parameters for a UMOT by comparing the capture ability of the DMOTs. Those two parameters will be helpful for a UMOT or multiple UMOT design on an atom chip. Furthermore, we demonstrate the mixing and splitting of the DMOTs with the help of an extra pair of anti-

Helmholtz coils on the atom chip. Our results also prove that trapping atoms in double or even more complex MOTs fabricated simultaneously on an atom chip can be performed directly from a background atomic vapor.

REFERENCES

1. R. Folman, P. Kruger, J. Schmiedmayer, J. Denschlag, and C. Henkel, "Microscopic atom optics: from wires to an atom chip," Adv. At., Mol., Opt. Phys. **48**, 263–356 (2002).
2. J. Fortagh and C. Zimmermann, "Magnetic microtraps for ultracold atoms," Rev. Mod. Phys. **79**, 235–289 (2007).
3. J. J. Hu and J. P. Yin, "Controllable double-well magnetic traps for neutral atoms," J. Opt. Soc. Am. B **19**, 2844–2851 (2002).
4. J. J. Hu, J. P. Yin, and J. J. Hu, "Double-well surface magneto-optical traps for neutral atoms in a vapor cell," J. Opt. Soc. Am. B **22**, 937–942 (2005).
5. M. Yun and J. P. Yin, "Controllable double-well magneto-optic atom trap with a circular current-carrying wire," Opt. Lett. **30**, 696–698 (2005).
6. M. E. Holmes, M. Tscherneck, P. A. Quinto-Su, and N. P. Bigelow, "Isotopic difference in the heteronuclear loss rate in a two-species surface trap," Phys. Rev. A **69**, 063408–063411 (2004).
7. M. Tscherneck, J. Kleinert, C. Haimberger, M. E. Holmes, and N. P. Bigelow, "Creating, detecting and locating ultracold molecules in a surface trap," Appl. Phys. B: Lasers Opt. **80**, 639–643 (2005).
8. J. Esteve, T. Schumm, J. B. Trebbia, I. Bouchoule, A. Aspect, and C. I. Westbrook, "Realizing a stable magnetic double-well potential on an atom chip," Eur. Phys. J. D **35**, 141–146 (2005).
9. M. Trupke, F. Ramirez-Martinez, E. A. Curtis, J. P. Ashmore, S. Eriksson, E. A. Hinds, Z. Moktadir, C. Gollasch, M. Kraft, G. V. Prakash, and J. J. Baumberg, "Pyramidal micromirrors for microsystems and atom chips," Appl. Phys. Lett. **88**, 071116–071118 (2006).
10. M. Singh, M. Volk, A. Akulshin, A. Sidorov, R. McLean, and P. Hannaford, "One-dimensional lattice of permanent magnetic microtraps for ultracold atoms on an atom chip," J. Phys. B **41**, 065301–065306 (2008).
11. P. Hommelhoff, W. Hansel, T. Steinmetz, T. W. Hansch, and J. Reichel, "Transporting, splitting and merging of atomic ensembles in a chip trap," New J. Phys. **7**, 3–19 (2005).
12. R. Dumke, M. Volk, T. Muther, F. B. J. Buchkremer, G. Birkl, and W. Ertmer, "Micro-optical realization of arrays of selectively addressable dipole traps: a scalable configuration for quantum computation with atomic qubits," Phys. Rev. Lett. **89**, 097903–097906 (2002).
13. R. Gerritsma, S. Whitlock, T. Fernholz, H. Schlatter, J. A. Luigjes, J. U. Thiele, J. B. Goedkoop, and R. J. C. Spreeuw, "Lattice of microtraps for ultracold atoms based on patterned magnetic films," Phys. Rev. A **76**, 033408–033413 (2007).
14. M. R. Andrews, C. G. Townsend, H. J. Miesner, D. S. Durfee, D. M. Kurn, and W. Ketterle, "Observation of interference between two Bose condensates," Science **275**, 637–641 (1997).
15. T. Schumm, S. Hofferberth, L. M. Andersson, S. Wildermuth, S. Groth, I. Bar-Joseph, J. Schmiedmayer,

and P. Kruger, "Matter-wave interferometry in a double well on an atom chip," Nat. Phys. **1**, 57–62 (2005).

16. Y. Shin, C. Sanner, G. B. Jo, T. A. Pasquini, M. Saba, W. Ketterle, D. E. Pritchard, M. Vengalattore, and M. Prentiss, "Interference of Bose–Einstein condensates split with an atom chip," Phys. Rev. A **72**, 021604–021607 (2005).

17. W. Hansel, J. Reichel, P. Hommelhoff, and T. W. Hansch, "Trapped-atom interferometer in a magnetic microtrap," Phys. Rev. A **64**, 063607–063612 (2001).

18. J. F. Bertelsen, H. K. Andersen, S. Mai, and M. Budde, "Mixing of ultracold atomic clouds by merging of two magnetic traps," Phys. Rev. A **75**, 013404–013414 (2007).

19. C. W. Chou, H. de Riedmatten, D. Felinto, S. V. Polyakov, S. J. van Enk, and H. J. Kimble, "Measurement-induced entanglement for excitation stored in remote atomic ensembles," Nature **438**, 828–832 (2005).

20. J. Laurat, C. W. Chou, H. Deng, K. S. Choi, D. Felinto, H. de Riedmatten, and H. J. Kimble, "Towards experimental entanglement connection with atomic ensembles in the single excitation regime," New J. Phys. **9**, 207–220 (2007).

21. L. M. Duan, M. D. Lukin, J. I. Cirac, and P. Zoller, "Long-distance quantum communication with atomic ensembles and linear optics," Nature **414**, 413–418 (2001).

22. Y. A. Chen, S. Chen, Z. S. Yuan, B. Zhao, C. S. Chuu, J. Schmiedmayer, and J. W. Pan, "Memory-built-in quantum teleportation with photonic and atomic qubits," Nat. Phys. **4**, 103–107 (2008).

23. S. Chen, Y. A. Chen, B. Zhao, Z. S. Yuan, J. Schmiedmayer, and J. W. Pan, "Demonstration of a stable atom-photon entanglement source for quantum repeaters," Phys. Rev. Lett. **99**, 180505–180508 (2007).

24. J. Reichel, W. Hansell, and T. W. Hansch, "Atomic micromanipulation with magnetic surface traps," Phys. Rev. Lett. **83**, 3398–3401 (1999).

25. S. Wildermuth, P. Kruger, C. Becker, M. Brajdic, S. Haupt, A. Kasper, R. Folman, and J. Schmiedmayer, "Optimized magneto-optical trap for experiments with ultracold atoms near surfaces," Phys. Rev. A **69**, 030901–030904 (2004).

26. B. Lev, "Fabrication of micro-magnetic traps for cold neutral atoms," Quantum Inf. Comput. **3**, 450–464 (2003).

27. X. L. Li, M. Ke, J. Y. Tang, S. Y. Zhou, S. Y. Zhou, and Y. Z. Wang, "Trapping of neutral Rb-87 atoms on an atom chip," Chin. Phys. Lett. **22**, 2526–2529 (2005).